Ground-state and optical properties of Cu_2O and CuO crystals

W. Y. Ching and Yong-Nian Xu*
Department of Physics, University of Missouri–Kansas City, Kansas City, Missouri 64110

K. W. Wong
Department of Physics and Astronomy, University of Kansas, Lawrence, Kansas 66045
(Received 7 March 1989)

The band structures of cubic Cu_2O and monoclinic CuO crystals have been calculated by means of the first-principles orthogonalized linear combination of atomic orbitals method. Using the wave functions obtained, the frequency-dependent interband optical conductivities are also evaluated. The results show Cu_2O to be a direct-gap semiconductor, while CuO is semiconductorlike with an intrinsic hole population at the top of the valence band (VB). By comparing with a variety of existing data, we conclude that band theory works extremely well for Cu_2O, but is less satisfactory for CuO. This could be due to strong correlation effects for states near the top of the VB in CuO. A careful reanalysis of optical data and excitonic spectra in Cu_2O in conjunction with our calculations suggests a complete reinterpretation of these data. A clear distinction between the intrinsic gap and the optical gap is argued. We conclude that the intrinsic gap in Cu_2O is of the order of 0.8 eV, while the optical gap is of the order 2.0–2.3 eV. The excitonic series in Cu_2O is due to the Coulombic attraction of the hole at the top of the VB and the electron in the next-higher conduction band (CB), not the lowest CB, because of the forbidden symmetry associated with angular-momentum conservation. This reinterpretation of the excitonic data is also consistent with a calculated low value for the static dielectric constant ϵ_0 of order of 4 for Cu_2O.

I. INTRODUCTION

Copper oxides exist in two stable forms, the cuprous oxide Cu_2O and the cupric oxide CuO. These two oxides have very different colors, crystal structures, and physical properties. Simple chemistry tells us that these differences are mainly due to the fact that Cu in Cu_2O is in the Cu^+ state, while Cu in CuO is in the Cu^{2+} state. Cu_2O is a red-colored cubic semiconductor that displays a wealth of interesting excitonic levels. CuO, on the other hand, has a dark, iron-gray color and crystallizes in a more complicated monoclinic tenorite structure exhibiting interesting antiferromagnetic ordering. Many different types of experiments have been carried out to determine various properties of these two forms of copper oxides. These include optical,[1–3] transport,[4–6] elastic,[7–9] plastic,[10] excitonic,[11–18] spectroscopic,[19–22] neutron scattering,[23] and many others.[24]

The recent discovery of high-temperature superconductivity[25] in ceramic oxides containing Cu has rekindled interest in studying the properties of copper oxides in much more detail. It has been suggested that the Cu valence and its fluctuation may be the key to understanding the mechanism for high-temperature superconductivity.[26] The valence of Cu in $YBa_2Cu_3O_7$ may be different depending on the crystallographic sites.[27] Since the oxidation states of Cu and O ions in Cu_2O and CuO crystals are very clear, it will be interesting to see if band theory can establish any correlations between effective charges on the ions and their oxidation states and elucidate the possible chemical bonding in these two crystals.

There have been several electronic-band-structure calculations on Cu_2O in the past.[28–30] Even long before the existence of any of these band calculations, the band concept was employed to stipulate the symmetry of the wave functions of excitons in Cu_2O.[31,32] On the other hand, little is known about the electronic structure of CuO. This is partly due to its more complicated crystal structure, but, more importantly, CuO may belong to that particular class of compounds known as Mott insulators, where conventional band theory generally fails. This has been the case with other transition-metal monoxides such as CoO and NiO.[33–35] However, the question as to what extent local-density theory (or local-spin-density theory) can adequately describe the Mott insulator has not been completely resolved and is still an actively pursued area of condensed-matter theory. It is therefore important and timely to study the electronic structures of these two copper oxides on an equal footing by using the same computational method in order to have a clearer picture of their ground-state properties.

In this paper we report the results of ground-state electronic-structure calculations on Cu_2O and CuO crystals using the state of the art, self-consistent orthogonalized linear combination of atomic orbitals method (OLCAO). In addition to the band structure and the density of states (DOS), we have also calculated the interband optical conductivity in these crystals so as to understand the excitation spectra as well. We shall compare our calculated results with different types of experimental data available and seek overall consistency in their interpretation. Based on our calculated results, some of these

 ©1989 The American Physical Society

long-standing data can now be interpreted differently.

The next section starts with a detailed discussion of the crystal structures. This is followed by the description of our calculation method in Sec. III. The main results on the ground-state properties are presented in Sec. IV, and those on the optical properties in Sec. V. These results are discussed together with relevant experimental observations in Sec. VI. Some concluding remarks are made in the last section.

II. CRYSTAL STRUCTURES

Cuprous oxide assumes a fairly simple cuprite structure,[36] as illustrated in Fig. 1(a). It can be best visualized as a cubic unit cell with a lattice constant of 4.2696 Å, such that the O ions are at the corners of the cube with a tetrahedral Cu_4O unit at the center, as illustrated in Fig. 1(a). Alternatively, it can be viewed as consisting of two interpenetrating frameworks of copper ions in a face-centered cube and oxygen ions in a body-centered cube that are not crosslinked by any primary Cu—O bonds. The cuprite structure has a high symmetry with space group O_h^4, the same as Ag_2O and Pb_2O oxides. Because of the low coordination number of 2 for the Cu atom, the O—Cu—O—Cu configuration appears as a zig-zag chain in the [110] direction with an unusually short Cu—O bond length of 1.85 Å. It is generally assumed that such a structure is indicative of covalent bonding between Cu and O. If complete ionic bonding is assumed, then exactly one electron is transferred from each Cu to O, resulting in the oxidation states Cu^+ and O^{2-}.

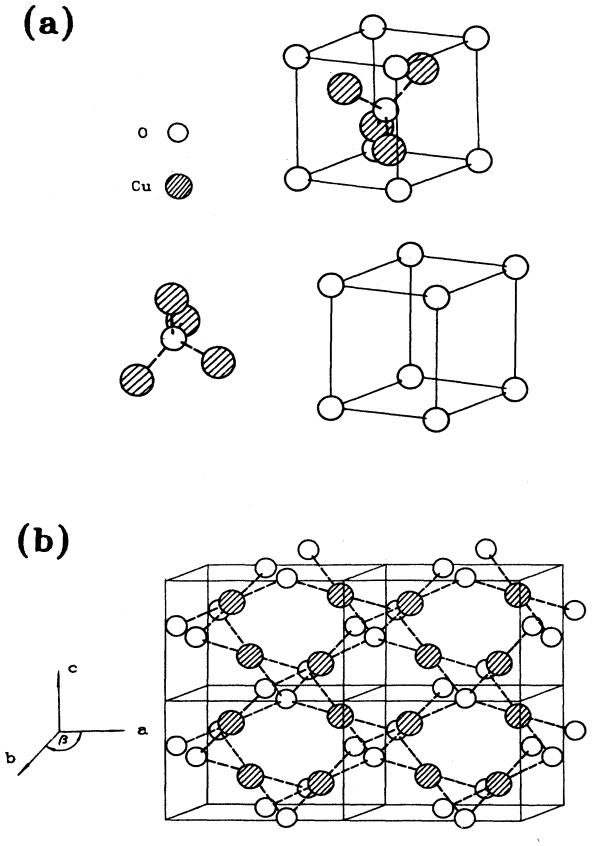

FIG. 1. Crystal structure of (a) cubic Cu_2O and (b) monoclinic CuO.

The cupric oxide CuO has a considerably more complicated tenorite structure,[37] similar to AgO. The monoclinic unit cell (space group C_{2h}^6) contains four CuO molecules. The crystal parameters were measured[38] to be $a=4.6837$ Å, $b=3.4226$ Å, $c=5.1288$ Å, and $\beta=99.54°$, as is illustrated in Fig. 1(b). The coordination of atoms in CuO is such that each ion has four nearest neighbors of the other kind. In the (110) plane, each Cu atom is linked to four nearly coplanar O atoms at the corner of an almost rectangular parallelogram. The Cu—O bond lengths in this plane are 1.88 and 1.96 Å, respectively, which are larger than those in the cuprous oxide. The next two Cu—O bond lengths perpendicular to the plane are much greater, so an octahedral type of coordination can be ruled out. The O atom is coordinated to four Cu atoms in the form of a distorted tetrahedron. It is generally believed that the bonding in CuO is a mixture of ionic and covalent bonding, although the oxidation state of Cu in CuO is unquestionably Cu^{2+}. The transition-metal monoxides such as CoO and NiO, on the other hand, crystallize in the rocksalt structure with much higher symmetry. Thus, this may indicate a fundamental difference in electronic states between the CuO crystal and those of NiO or CoO.

III. METHOD OF CALCULATION

We have used the self-consistent orthogonalized linear combination of atomic orbitals method within the local-density approximation to calculate the band structures of Cu_2O and CuO. The details of the method have been described in the literature.[39,40] It has been shown that highly accurate ground-state properties for diamond Si (Ref. 40) and wurtzite AlN (Ref. 41) can be obtained by this method. Within the past two years this method has also been extensively used to calculate the band structures and interband optical conductivities of a number of newly discovered oxide superconductors.[42–45] We shall outline the procedures used in the present study for Cu_2O and CuO crystals.

In the OLCAO method the basis functions are atomic-like functions calculated separately and expressed as a linear combination of Gaussian-type orbitals. We used a set of 16 Gaussians per atom with exponentials ranging from 0.15 to 50 000 to form Cu $1s, 2s, 3s, 4s, 5s, 2p, 3p, 4p, 5p, 3d, 4d$ and O $1s, 2s, 3s, 2p, 3p$ atomic wave functions. This is referred to as a full basis set because it consists of the atomic orbitals of all the valence-shell electrons (both occupied and unoccupied) plus an extra shell of unoccupied states. Past experience indicates that such a full basis can provide sufficient variational freedom for the Bloch function. The valence and the empty orbitals at each atomic site were then orthogonalized to all the core orbitals of all the atoms in the cell such that the core states are eliminated

in the solution of the secular equations.[46] This procedure greatly reduces the computational time because of the reduction of the dimension of the secular equations. The eliminated core states (Cu $1s, 2s, 3s, 2p, 3p$ and O $1s$) are of no interest in the present study.

In the self-consistent calculation, both the potential and the charge-density functions were also expanded in terms of a set of simple Gaussians centered at each atomic site. The coefficients of this expansion were obtained by numerically fitting the data calculated at a large number of real-space sampling points. The exponentials α of this Gaussian basis set were predetermined. We have adopted a set of 16 Gaussians per site with α ranging from 0.5 to 10 000 000, distributed according to a geometric series. Since the charge-density distributions in both Cu_2O and CuO are nearly spherical around each atom, no auxiliary sites were employed for the potential and charge-density fitting, as was done in the case of Si (Ref. 40) and AlN (Ref. 41). The accuracy of the calculation depends on the quality of the fit, which must be closely monitored. The errors associated with an unconstrained fit in the present calculation were 0.000 67 and 0.000 06 electrons per valence electron for Cu_2O and CuO, respectively. Such a fitting accuracy is generally adequate for the band-structure and wave-function studies, but may not be sufficient for obtaining accurate total ground-state energies.[40,41,47]

The Brillouin-zone (BZ) integration for the charge-density calculation in the self-consistent iterative procedure was based on 12 special $\mathbf{k}$ points in the irreducible part of the zone. The exchange and correlation potentials were approximated by the Wigner interpolation formula. Fifteen to eighteen iterations were needed to achieve self-consistency. The energy eigenvalues stabilized to less than 0.000 01 eV when convergence was reached. The energy eigenvalues and eigenfunctions were then solved at 149 regularly spaced $\mathbf{k}$ points in the irreducible part of the BZ for Cu_2O (CuO), from which the densities of states (DOS's) were calculated using the linear analytical tetrahedron method.[48] The partial DOS (PDOS) and the effective charge of each atom were evaluated by the Mulliken charge-analysis procedure.[49]

The optical properties of these two crystals were studied as follows. First, the real part of the interband optical conductivity $\sigma_1(\omega)$ in the random-phase dipole approximation was evaluated according to

$$\sigma(E)=\frac{2\pi e^2}{3m^2E\Omega}\frac{\Omega}{(2\pi)^3}\int_{\mathrm{BZ}}d\mathbf{k}\sum_{n,l}|\langle\psi_n(\mathbf{k},\mathbf{r})|\mathbf{P}|\psi_l(\mathbf{k},\mathbf{r})\rangle|^2 f_l(\mathbf{k})[1-f_n(\mathbf{k})]\delta(E_n(\mathbf{k})-E_l(\mathbf{k})-E)\ , \tag{1}$$

where $E=\hbar\omega$ is the photon energy. The momentum matrix elements (MME's) at each $\mathbf{k}$ point in the BZ were evaluated exactly without any approximation, and the transition probability was averaged over the three Cartesian directions. $\sigma_1(\omega)$ was calculated up to a photon energy of 20 eV. The integration of (1) over the BZ was again carried out by using the analytic linear tetrahedron method.[48] The matrix-element contribution from each tetrahedral microzone was taken as the average of the MME at the four corner points of the microzone. Accurate evaluation of MME's has been of crucial importance in obtaining an accurate optical conductivity function. In principle, evaluation of the MME can be incorporated into the linear analytic tetrahedron method.[50] However, with a sufficient number of $\mathbf{k}$ points in the BZ, the averaging procedure for the MME contribution was found to be adequate. Next, the imaginary part of the dielectric function $\epsilon_2(\omega)$ is obtained from $\sigma_1(\omega)$ through $\epsilon_2(\omega)=(4\pi)\sigma_1(\omega)/\omega$, and the real part of the dielectric function is obtained from $\epsilon_2(\omega)$ through the Kramers-Kronig relation. From the dielectric function $\epsilon(\omega)=\epsilon_1(\omega)+i\epsilon_2(\omega)$, the refractivity spectrum can also be obtained.

IV. RESULTS ON GROUND-STATE PROPERTIES

A. Cu_2O

The band structure of Cu_2O calculated by the OLCAO method is shown in Fig. 2 along the directions of the symmetry axes of the BZ. It shows Cu_2O to be a semiconductor with a direct band gap of 0.78 eV at Γ. The valence band (VB) consists of two parts. The upper part has a width of about 4 eV and consists predominantly of Cu $3d$ states. The lower part, which is about 3.5 eV wide, contains a significant number of O $2p$ states. These two parts are separated by a direct gap at Γ 0.8 eV. There have been several band-structure calculations on Cu_2O. The earlier calculations[28,29] were much less accurate simply because the computational methods of modern band

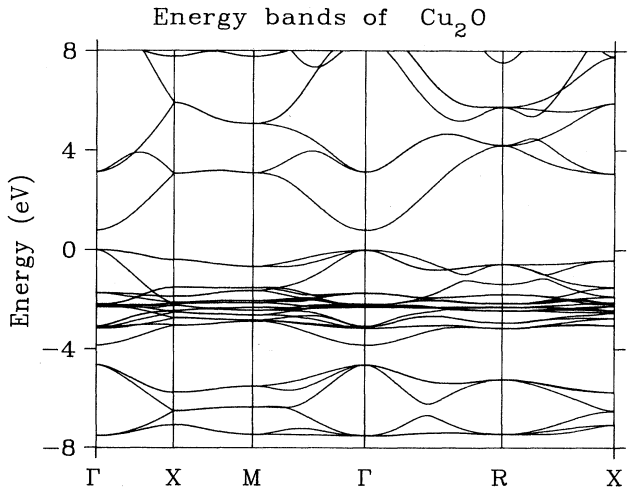

FIG. 2. Band structure of Cu_2O.

theory had not been fully developed. The most recent calculation was carried out by Kleinman and Mednick[30] (KM), who also studied the spin-orbit splitting of the states at the top of the VB. Our results on both the VB and the conduction band (CB) are close to those of KM, who obtained a gap value of 1.07 eV. This value is larger than ours, but is still smaller than the oft-quoted experimental value of 2.04 eV. It is well known that local-density calculations always underestimate the band gap of a semiconductor, but, in the case of Cu_2O, the size of the gap will not be settled until a much more careful analysis of the optical data is performed. We will return to this point in Sec. VI, in which the calculated and measured optical properties are compared.

The calculated DOS and the orbital-projected PDOS for Cu_2O are displayed in Fig. 3. It is clear that the VB is dominated by the Cu $3d$ states. Cu $4p$ and Cu $3s$ states are only negligible components, while O $2s$ states are almost entirely absent. The DOS of Cu_2O has a rich spectrum with multiple structures. The most prominent ones are at -0.06, -2.38, and -3.05 eV for the upper VB and at -5.57 and -7.46 eV for the lower VB. The CB also has several structures that are much less prominent than those of the VB. It is important to note that the DOS at the bottom of the CB is very small and rises gradually as the energy is increased. We will compare our calculated DOS spectrum with the experimental photoemission measurement in Sec. VI.

The components of effective electron and hole masses for Cu_2O along different symmetry directions at Γ are summarized in Table I. In the absence of spin-orbit splitting, the states at the top of the VB at Γ are triply degenerate. The electron effective mass is very isotropic, while the hole effective masses are not. The top two VB's are much heavier than the third band. The anisotropy in the hole effective masses is evidenced by their very different components in the [100], [110], and [111] directions. They range from $-0.34m$ for the lowest band in the [100] direction to $-3.16m$ for the top band in the same direction. By averaging over all directions, we obtain the electron effective mass of $0.66m$ and the hole effective masses of $-3.02m$, $-1.41m$, and $-0.50m$ for Cu_2O. This corresponds to averaged reduced masses between electrons and holes of $0.54m$, $0.45m$, and $0.28m$, respectively. Therefore, on the average, the effective reduced mass between a top of a VB hole and a lowest CB electron in Cu_2O is about $0.42m$. The reduced effective mass corresponds to the excitonic mass, and its accurate determination is of crucial importance in interpreting the excitonic levels.

In Fig. 4 we display the valence charge-density distribution on the (110) plane. It can be seen that the charge distribution is almost confined to the Cu—O—Cu—O zig-zag chains in this plane. Around both Cu and O ions the distribution is nearly spherical with no evidence of bond charge. This is illustrated more clearly in Fig. 5, in which the electron density $\rho(r)$ along the Cu—O bond direction is plotted. Thus the charge distribution appears

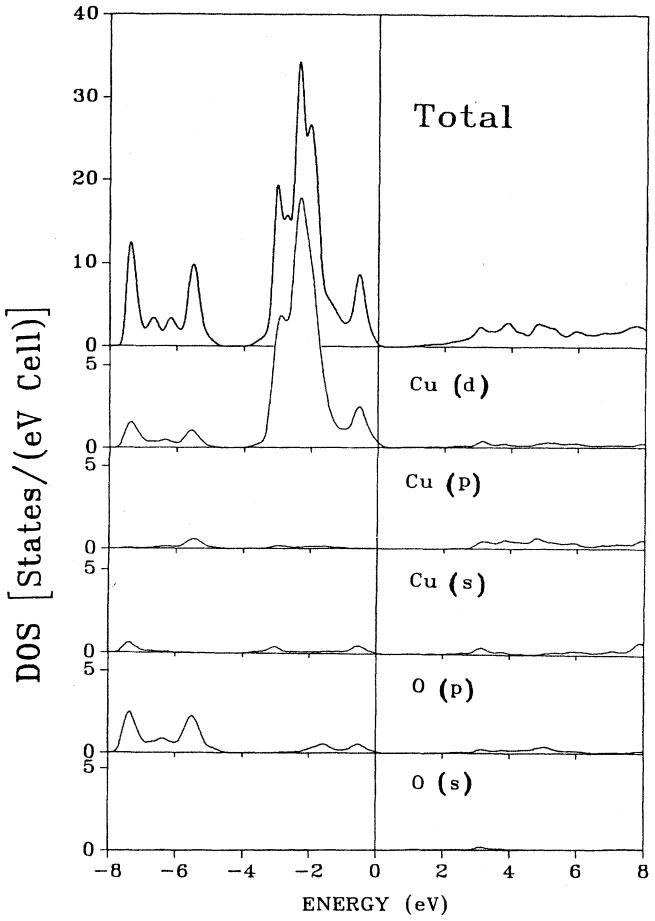

FIG. 3. Calculated DOS and PDOS of Cu_2O.

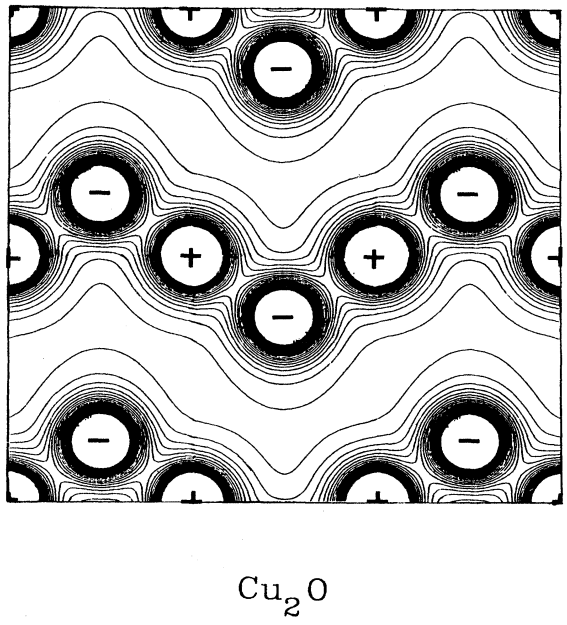

FIG. 4. Valence charge-density distribution of Cu_2O in the (110) plane.

TABLE I. Effective-mass components at Γ for Cu_2O (in unit of m).

CB	0.65	0.66	0.66
	−3.16	−3.14	−2.74
VB	−3.16	−1.02	−0.67
	−0.34	−0.46	−0.67

to suggest that Cu_2O should be quite ionic. However, a Mulliken charge analysis gives the following distribution of valence electrons on each ion: Cu $3d$, 9.98; Cu $4s$, 0.59; Cu $4p$, 0.50; O $2s$, 1.72; O $2p$, 4.15. This translates into effective charges Q^* of 11.07 and 5.87 electrons for Cu and O ions, respectively, and thus shows no evidence of charge transfer. A more accurate estimation by means of direct integration over a spherical region of radius $r=0.924$ Å for both Cu and O (indicated by a vertical arrow in Fig. 5) gives $Q^*_{Cu}=10.42$ electrons and $Q^*_O=6.57$ electrons with 1.18 electrons in the interstitial region of the cell. Hence the charge calculation does not support the fully ionic picture for Cu_2O, in which each Cu ion transfers one electron to O to form O^{2-}.

B. CuO

We are not aware of any existing band-structure calculation for cupric oxide. As alluded to in the Introduction, our purpose in calculating the band structures for CuO is to test the validity of the local-density theory for this unique system and for making a parallel comparison with the Cu_2O crystal. Our calculated band structure for CuO using the OLCAO method along the symmetry axes of the monoclinic BZ is shown in Fig. 6. This band structure is drastically different from that of Cu_2O. First, it has a semiconductor-like structure with a direct gap of 1.60 eV at Γ. This value is quite close to the reported gap values of 1.7 eV (Ref. 51) and 1.4 eV (Ref. 52) obtained by using indirect electrochemical methods on polycrystalline samples. However, our calculation shows that a Fermi surface is present, thus resulting in the existence of exactly four intrinsic holes at the top of the VB. It is interesting to note that the high-T_c superconductor $YBa_2Cu_3O_7$ also has four intrinsic holes at the top of the VB.[42] The top of the VB at Γ is 0.95 eV above E_F, and the bottom of the CB is 2.55 eV above E_F. The VB is about 8.5 eV wide and does not have a second gap as in the case of Cu_2O.

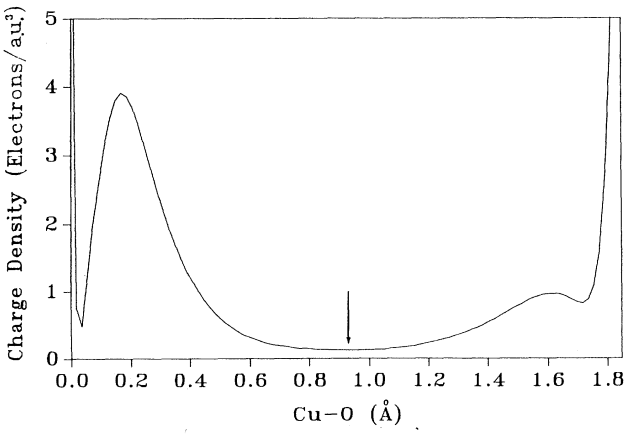

FIG. 5. Charge density $\rho(r)$ along the Cu—O bond in Cu_2O. The arrow defines the radii of the touching spheres for charge integration.

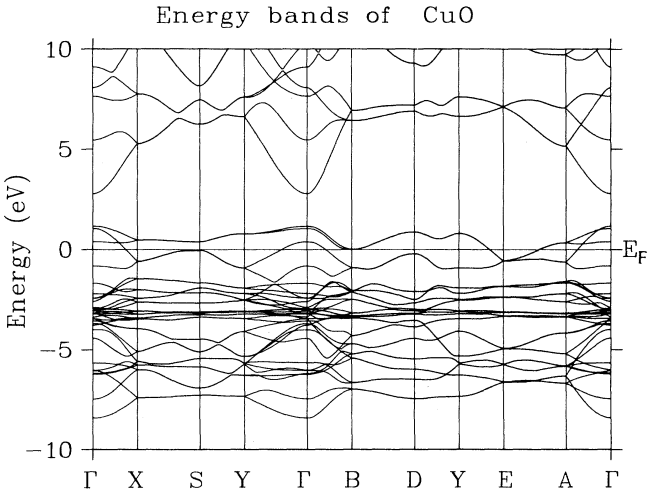

FIG. 6. Band structure of CuO.

Figure 7 displays the DOS and PDOS spectra for CuO. In the VB the states are dominated by the Cu $3d$ and O $2p$ components. The most prominent structure is at −3.20 eV. The second most visible structure is at −6.04 eV. Other structures at −0.89, −1.92, −2.47, −4.72, and −7.08 eV can also be identified. For the unoccupied states a rather sharp peak at 0.58 eV near the top of VB is evident and the CB has a broad peak at 7.37 eV. The major peak at −3.20 eV in the VB is almost exclusively derived from Cu $3d$ states. For other peaks in the VB, including that from the intrinsic hole states, both Cu $3d$ and O $2p$ states participate. The value of the DOS at the Fermi level for CuO is 3.72 states/eV cell.

The effective-mass components for bands at Γ in CuO along several crystallographic directions are listed in Table II. The effective mass of the CB is no longer isotropic because of the noncubic crystal structure. In the

TABLE II. Effective-mass components at Γ for CuO (in unit of m).

	direction			
	$[\Gamma=>X]$	$[\Gamma=>Y]$	$[\Gamma=>B]$	$[\Gamma=>A]$
CB	0.42	0.46	0.16	0.37
VB	−1.75	−3.01	−0.60	−0.54
	−0.72	−3.72	−0.58	−1.33

CB the effective mass is lighter in the z direction than in the x or y directions. For the VB the component in the y direction is unusually heavy. At the Γ point the top two bands are very close to each other. At the Γ point the hole effective mass has components $-1.75m$, $-3.01m$, $-0.60m$, and $-0.54m$ along the $\Gamma-X$, $\Gamma-Y$, $\Gamma-B$, and $\Gamma-A$ directions. For the second band, the corresponding components are $-0.72m$, $-3.72m$, $-0.58m$, and $-1.33m$. Therefore, in both Cu_2O and CuO, the hole effective masses are heavier than the electron effective mass.

Figure 8 displays the valence charge-density distribution of CuO in the (110) plane containing the CuO_4 unit. Again, the distribution is nearly spherical for both types of ions, with no evidence of bond charge between the two. The charge-density distribution along a Cu—O bond, shown in Fig. 9, is similar to that of Fig. 5 for Cu_2O. The only difference is that the Cu—O bond in Fig. 8 is 1.947 Å long instead of 1.849 Å as in Fig. 5. Mulliken charge analysis gives the following effective charges: Cu $4s$, 0.52; Cu $4p$, 0.66; Cu $3d$, 9.79; O $2s$, 1.75; O $2p$, 4.27. This gives a total effective charge Q^* of 10.97 electrons for Cu and 6.02 electrons for O. Like Cu_2O, these numbers show little or no charge transfer. Real-space spherical integration with a radius 0.966 Å for both ions gives $Q^*_{Cu}=10.52$ electrons and $Q^*_O=6.72$ electrons, which overestimates the total charge within the cell by about one electron. From these calculations it appears that it is difficult to assign definitive values for valence charges to both of the ions in CuO and Cu_2O crystals, indicating the bonding in these two crystals is neither ionic nor covalent. These conclusions are based on the fact that radii of the Cu and O ions are both equal to half of the bond length, as indicated by the arrows in Figs. 5 and 9. It is unlikely that improved numerical accuracy will yield

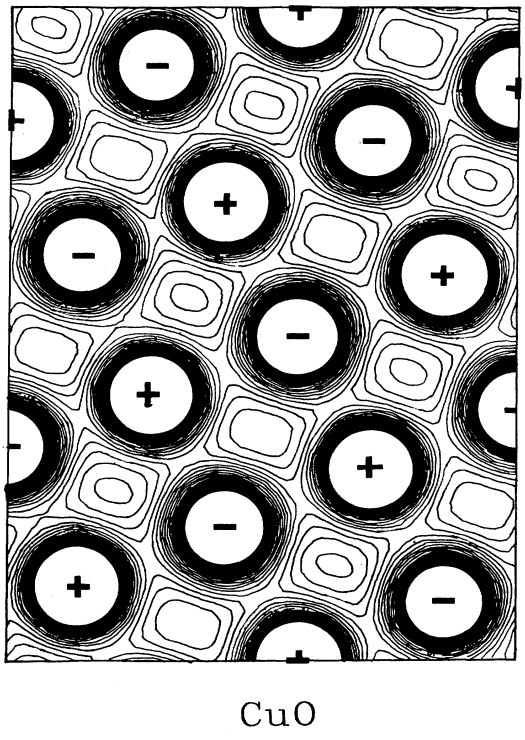

FIG. 8. Valence charge-density map of CuO in the (110) plane.

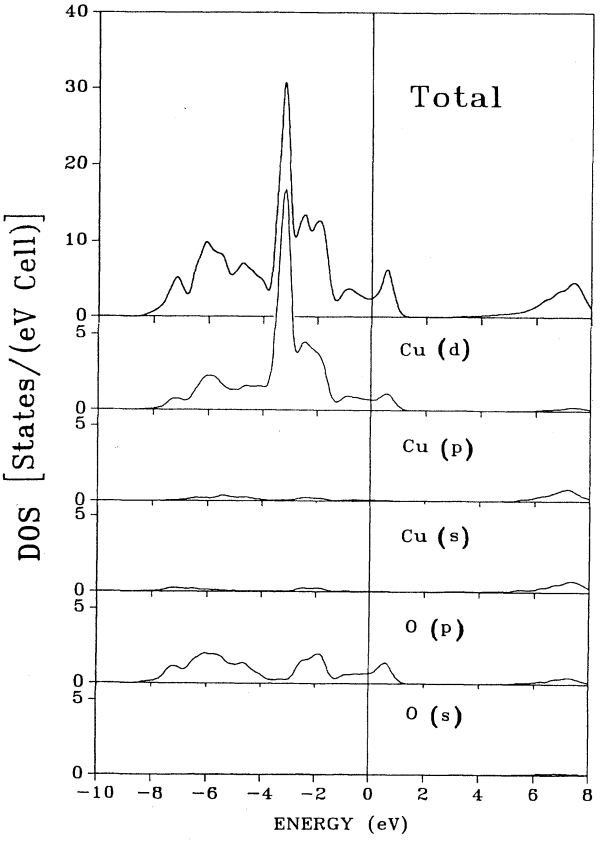

FIG. 7. Calculated DOS and PDOS of CuO.

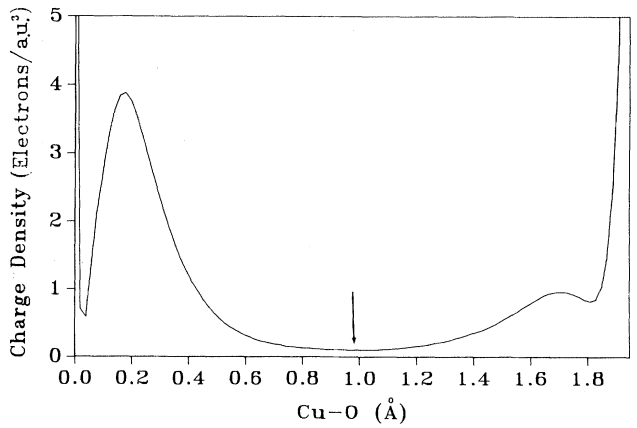

FIG. 9. Charge density $\rho(r)$ along the Cu—O bond in CuO. The arrow defines the radii of the touching spheres for charge integration.

numbers significantly different from the two estimates given above. Apparently, effective charge per atom is an ill-defined concept in copper oxides that has no direct bearing on the oxidation states of the ions in the crystal.[27]

V. RESULTS ON THE OPTICAL PROPERTIES

The interband optical conductivity for Cu_2O calculated according to Eq. (1) is shown in Fig. 10(a). Although the calculated band gap for Cu_2O is 0.76 eV, the optical absorption is negligible in the low-energy range up to 2.6 eV. This is a source of difficulty for a direct measurement of the band gap by optical means, and indicates that the symmetry of the wave functions near the band edge is such that a direct transition at Γ is forbidden. Elliott[31] was the first to point out the forbidden dipole transition in Cu_2O based on a detailed group-theoretical analysis. Inspection of eigenfunctions for the triply degenerate states at the top of the VB shows that these wave functions contain no O s component, but contain the O p components as well as the Cu s and Cu d orbitals, while the bottom of the CB is dominated by the O s orbitals, with substantial mixing from the Cu s and Cu d orbitals, but none from the O p orbitals. Both states have no Cu p components. At first sight, one would like to argue that the s-p matrix element should be nonzero in such a transition. However, the unit cell contains two Cu_2O molecules, and the relative phases of the Bloch functions are such that the transition is forbidden at the zone center. The absorption starts to become significant for photon energies above 3.2 eV because a transition to the next-higher CB states or for states along the $X-M$ direction becomes possible. At Γ, the next-higher CB (doubly degenerate), the Bloch states consist entirely of Cu p orbitals. The major structures in the $\sigma(E)$ curve for Cu_2O are at 3.79, 4.55, and 5.20 eV (labeled A, B, and C, respectively), while the two minor structures (labeled E and F) are at 4.03 and 4.94 eV. These structures can be accounted for by specific band-to-band transitions. Peak A originates from transitions involving the top VB states to the first CB state along the $X-M$ direction while peak C involves transitions from the lower VB states to the same first CB in the same direction. Peak B can be traced to the transitions between a pair of almost parallel bands in the $R-X$ direction. The big drop in $\sigma(E)$ between peaks B and C is the reflection of the two leading peaks in the VB DOS at -0.60 and -3.05 eV mentioned in Sec. IV A. Above 5.7 eV there are multiple structures in $\sigma(E)$ involving a more complicated pattern of transitions. We will discuss these structures again in the next section, together with available data from optical measurements.

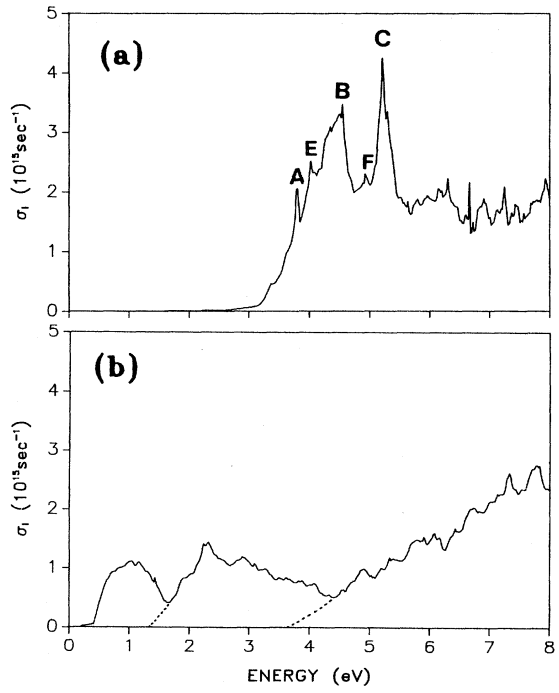

FIG. 10. Interband optical conductivity $\sigma_1(\omega)$ for (a) Cu_2O and (b) CuO. Dotted lines in (b) show possible absorption edges.

A similar interband optical calculation has been carried out for the CuO crystal. We have assumed that transitions from the states below E_F to the empty hole states near the top of VB are possible. Since one-electron theory may not be fully applicable for a system like CuO, this assumption ignores any possible correlation that may be quite strong in the CuO crystal. The interband conductivity of CuO is shown in Fig. 10(b), which is much different from that of Cu_2O in Fig. 10(a). The absorption strength is generally smaller, and the spectrum lacks sharp structures, as would be expected from a crystal of low symmetry. Although a Fermi surface exists in CuO, absorption becomes significant only for photon energies greater than 0.4 eV. It reaches a broad maximum at 1.0 eV, then drops to a minimum at 1.7 eV and reaches another broad maximum at 2.3 eV. The first broad maximum in $\sigma(E)$ is obviously from the transition below E_F to the empty intrinsic hole states near the top of the VB. The minimum at 1.7 eV is, of course, the signature of the semiconductor-like gap discussed previously. After reaching another broad minimum at 4.4 eV, $\sigma(E)$ increases gradually as a function of photon energy. Because the band structure of CuO is considerably more complicated due to its low crystal symmetry, it is difficult to make specific assignments of band-to-band transitions in CuO.

The real and imaginary parts of the dielectric functions extracted from the interband optical conductivity curves and the Kramer-Kronig relation are shown in Figs. 11(a) and 11(b) for Cu_2O and CuO, respectively. The structures in the $\epsilon(E)$ curves can be traced to the structures in the $\sigma(E)$ curves and they will not be discussed in detail. Of more importance is the value of the static dielectric constant $\epsilon_0=\epsilon_1(0)$. We obtained $\epsilon_0=3.7$ for Cu_2O and 12.3 for CuO. These two ϵ_0 values are to be compared with the experimentally determined values of 7.5 (Ref. 6) and 12.0 (Ref. 53), respectively. It appears that for Cu_2O the calculated value is only about half the measured one.

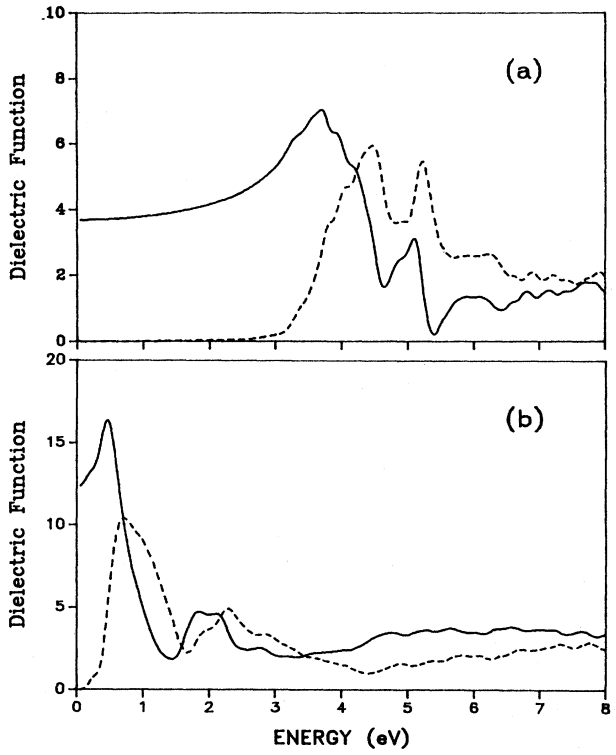

FIG. 11. Real (solid line) and imaginary (dashed line) parts of the frequency-dependent dielectric function derived from the conductivity function: (a) Cu_2O and (b) CuO.

However, we must remember that the experimental value is most likely deduced from the optical data, which inevitably involve other parameters such as the optical gap and the reduced effective mass. A small ϵ_0 value for Cu_2O is not inconsistent with revised values for these parameters. It is also noteworthy that, although CuO has a Fermi surface, and therefore will normally be regarded as a metal, its calculated value of ϵ_0 is comparable to those of semiconductors such as Si and GaAs with ϵ_0 values of 11.5 and 15.9, respectively. The ϵ_0 value for CuO will be even smaller if one only considers the interband transitions from the occupied portion of the VB to the CB. Thus, based on the magnitude of ϵ_0, CuO should be regarded as a semiconductor-like material and not a metal, in agreement with experimental observations.

VI. DISCUSSION AND COMPARISON WITH EXPERIMENTS

Our band-structure calculations for Cu_2O show it to be a semiconductor with a direct band gap of 0.78 eV at Γ, much smaller than the oft-quoted experimental gap value of 2.2 eV. One would tend to reconcile this difference as being due to the fact that local-density calculations generally underestimate the gap because of a failure to include self-interaction corrections or other types of many-body corrections necessary for obtaining the correct excited states. However, we believe that, in the case of Cu_2O, the experimentally determined E_g is actually the optical gap, while the band-structure calculation gives the intrinsic gap. These two entities are definitely not the same. As can be seen from the optical calculation of Sec. V, the direct transition at Γ is symmetry forbidden, and the optical absorption in Cu_2O becomes appreciable only at photon energies above 2 eV. In fact, the calculated intrinsic gap value is very close to the reported activation energy of 0.65 eV (Ref. 5) or 0.767 eV (Ref. 4). Whether this activation energy involves intrinsic conduction or transitions to impurity states near the CB edge has not been completely clarified. Nevertheless, these activation-energy values are certainly consistent with our calculated value of the intrinsic gap. Although the accuracy of the calculated value is somewhat affected by the local-density approximation and the numerical procedure associated with the OLCAO method, we believe that the intrinsic gap in Cu_2O should be much smaller than the optical gap determined experimentally. The reported hole effective mass of Cu_2O is $0.84m$,[6] which is close to the calculated values ranging from $0.46m$ to $1.02m$ for the lighter bands along the [110] and [111] directions.

The band structure of CuO turns out to be most interesting. The existence of intrinsic hole states at the top of the VB is consistent with the reported p-type conductivity in CuO.[54] An interesting experimental measurement of resistance in CuO as a function of pressure showed a discontinuous drop of 4 orders of magnitude at 391 K at a pressure of 187 kbar, which was not observed in other transition-metal oxides.[7] This was explained as being indicative of the occurrence of some type of pressure-induced phase transition in CuO. It is conceivable that at such a high pressure the semiconductor-like gap shown in Fig. 5 may collapse, transforming CuO into a normal metal. It has been suggested,[22] however, that CuO belongs to the category of binary transition-metal oxides generally characterized as Mott insulators, such as CoO or NiO. For such compounds the prevailing consensus appears to be that one-electron band theory is inadequate to describe the ground-state electronic structure. Thus our calculation for CuO is to be considered exploratory rather than confirmatory. Spin-polarized band-structure calculations[34] for NiO showed E_F to lie in a small gap, in contrast to a finite DOS at E_F in the present calculation. Neutron-scattering studies[23] on CuO crystals indicated antiferromagnetic ordering at 220 K with a moment of $0.68\mu_B$ per Cu, which is significantly smaller than $1.81\mu_B$ for Ni in NiO. It is not clear to what extent this magnetic ordering will affect the ground-state electronic structures of CuO. These differences and the fact that CuO has a much more complicated monoclinic structure tend to suggest that CuO may belong to a different category than the usual transition-metal oxides.

Optical measurements on cuprous oxide in the ultraviolet region have been performed.[1] The spectra were interpreted in terms of whatever band-structure information was available at the time. Our first-principles calculation of optical properties presented above makes interpretation of such data much easier. In Fig. 12 we compare the measured and the calculated $\epsilon_2(\omega)$ curves for

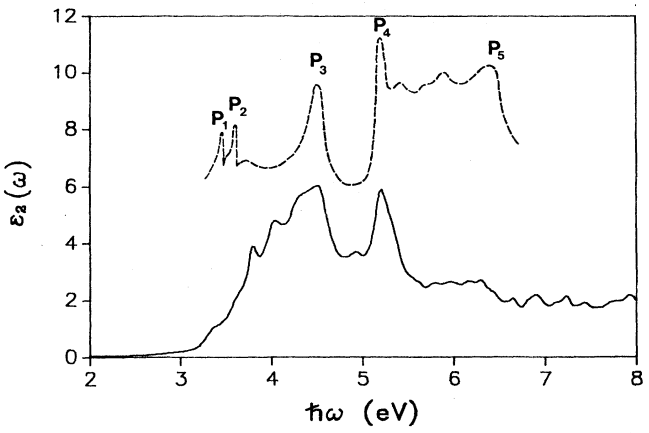

FIG. 12. Comparison of the experimental (Ref. 1) and the theoretical $\epsilon_2(\omega)$ curves. A shift of about 1 eV for the experimental curve has been applied.

Cu_2O. The experimental curve is shifted by about 1 eV to make the peak structures align. Five prominent structures in the experimental curve, labeled $P1$, $P2$, $P3$, $P4$, and $P5$, can be identified. The first two peaks, $P1$ and $P2$, at 2.54 and 2.69 eV, were interpreted to result from a transition to the excitonic levels.[13,14] Peaks $P3$ and $P4$, at 3.58 and 4.34 eV, were attributed to band-to-band transitions. $P5$ at 5.43 eV is really a sharp edge beyond which the absorption drops rapidly. To our surprise, other than the exciton-related peaks $P1$ and $P2$ all other structures were reproduced by the theoretical calculation, although an overall shift in the theoretical curve was needed. The need for such a shift could be of experimental origin related to the gap determination, or it could be due to the presence of excitonic levels which, in turn, may affect the optical spectrum. Nevertheless, the close agreement in the calculated $\epsilon_2(\omega)$ curve with the measured one cannot be considered as fortuitous, especially when the relative separations of the peak positions are so very close. The experimental separation between $P3$ and $P4$ is 0.76 eV. The range of the plateau from $P4$ to the edge $P5$ is 1.09 eV. The calculated values for these two separations are 0.76 and 1.08 eV, respectively. The big minimum between $P3$ and $P4$ that was discussed earlier in the $\sigma_1(E)$ curve is also well reproduced. Some additional small structures between $P4$ and $P5$ are also visible. The most unmistakable signature of the spectrum is the huge minimum between $P3$ and $P4$, which was well reproduced by the calculation.

The above discussion tends to support the earlier conclusion that the intrinsic gap in Cu_2O should be much smaller than the long-quoted value of nearly 2.2 eV, since a shift to the lower transition energy is required to align the calculated peaks with the experimental ones. However, it is also conceivable that the energy scale in the experimental curve was not accurately determined. Therefore, more accurate optical measurements with single-crystal Cu_2O are called for. As discussed earlier, the direct dipole transition is forbidden by the selection rules between the Bloch states of the CB and VB edges. The same selection rules also forbid the excitonic-state $n=1$ (s state) transition to the O p state in the VB. This feature is confirmed by the missing $n=1$ line of the excitonic yellow series[12] in Cu_2O. The excitonic spectrum is given by

$$\nu_n=\nu_\infty-R'/n^2,\quad n=1,2,3,\ldots \tag{2}$$

where R' is the effective Rydberg constant given by $R'=R(\mu^*/m_e)/\epsilon_0^2$, and R is the hydrogen Rydberg constant. μ^* is the excitonic reduced mass and ϵ_0 is the interband static dielectric constant. ν_∞ was experimentally determined to be 2.164 eV by fitting to the excitonic Rydberg series.[12] This threshold frequency is the same as the value obtained from the optical-absorption edge. It is likely that it is the optical gap, because the same selection rules that govern the forbidden dipole transition between the CB O s electronic state to the VB O p electronic state also govern the excitonic s state to the VB O p state. If the formation of the excitonic states is due to the Coulomb binding between the VB O p hole state and the lowest CB O s state, then it follows from the angular-momentum addition that no total $L=0$ state can be obtained, and thus the $n=1$ state must be absent in such an exciton. In the yellow series it was observed experimentally[12] that a quadrupole transition occurs that reveals the presence of the $n=1$ excitonic level. We can therefore conclude that the yellow excitonic series comes from the binding between the O p VB hole state with the next-higher CB state, which is dominated by the Cu p orbitals. If this is the case, ν_∞ in (2) is the same as the optical gap, which is close to the second-lowest CB at Γ, not the intrinsic gap. Gross[12] had actually pointed out the possibility of having exciton lines in the higher-CB spectrum. The unavailability of a realistic band structure for Cu_2O had prevented previous researchers from making a more precise interpretation.

Our new interpretation of the yellow excitonic spectra also leads to a significantly different interpretation of what constitutes the excitonic effective mass. Although the O s CB effective mass is quite well defined and rather isotropic, as discussed in Sec. IV A, the Cu p CB electron is not as isotropic. Like the VB O p state, its effective mass ranges from $0.20m$ to $0.53m$ depending on which state is at Γ. The excitonic reduced mass between one of the O p states in the VB and one of the p states in the CB can range from $0.12m$ to $0.48m$. Hence, from the excitonic spectra, we can easily deduce the interband dielectric constant ϵ_0 to range from 3.7 to 7.4, which is consistent with the calculated value from the interband optical conductivity. Had we used the μ^* value deduced from the lowest-CB effective mass, the ϵ_0 value would be considerably larger. Therefore, it is our belief that the experimental data on the excitonic spectra are consistent with a small direct intrinsic gap of 0.8 eV and a small dielectric constant of about 4 for Cu_2O. Both excitonic and optical spectra involve transitions from the top of the VB to the next-higher CB rather than to the lowest CB.

We are not aware of any direct optical measurement on

single-crystal CuO samples. Koffyberg and Benko[52] made a photoelectrochemical determination of the CB and VB edges in a lithium-doped p-type CuO polycrystal. By relating the energy dependence of the quantum efficiency η to the optical-absorption coefficient, they have identified two well-defined absorption edges at 1.35 and 3.25 eV and a small maximum at 1.17 eV. The first edge was interpreted as the indirect gap and the second as arising from direct transitions from the low-lying O states to the CB, while the occurrence of the small maximum was unexplained. These data are not inconsistent with our optical calculation based on first-principles band structure. In the $\sigma_1(E)$ curve for CuO [Fig. 10(b)], if we extrapolate the edges at the two minima as indicated by the dotted lines in Fig. 10(b), they intercept the energy axis at 1.3 and 3.6 eV, close to the observed edges. The unexplained small maximum can be identified as the first broad maximum at 1.0 eV in Fig. 10(b), which arises from the transitions from the states below E_F to the unoccupied intrinsic hole states. However, because of the strong correlation effects in CuO for states near the gap, and the fact that the experimental measurement was not a direct optical measurement on well-characterized samples, it is premature to draw a more definitive conclusion. Many of the band assignments for CuO in Ref. 52 remain tentative because of the unavailability of reliable band structure at that time.

Photoemission experiments on copper oxides have been performed by several groups.[19,20] The most recent and detailed study was done by Ghijsen and co-workers.[22] They have studied the electronic structures of both Cu_2O and CuO by x-ray photoemission spectroscopy (XPS), ultraviolet photoemission spectroscopy (UPS), and Auger-electron spectroscopy for the VB and the core levels and by bremsstrahlung isochromat spectroscopy (BIS) for the CB. They have concluded that the experimental data were consistent with band theory in the case of Cu_2O, but disagreed with the band result in the case of CuO because of strong correlation effects. We shall compare our results with their measurements. In Fig. 13(a) we compare our broadened total DOS (convoluted with a Gaussian of 0.3 eV) with the UPS data with a He II source. These particular data are chosen for comparison because, for He II, the O $2p$ and Cu $3d$ photoionization cross sections are comparable, so that the measured count is directly proportional to the total VB DOS without the need for additional scaling in the calculated DOS. The leading peak at -1.2 eV in the theoretical curve is shifted by 0.65 eV so as to align with the experimental one. As can be seen, there is excellent agreement in the two DOS spectra. All the peaks are reproduced, especially the major peak at -3.0 eV and the double peak in the -6 to -8 eV range. Furthermore, the presence of a shoulder at -3.7 eV is also quite evident.

A similar comparison for CuO is presented in Fig. 12(b). Here the agreement is less satisfactory. After a shift of 0.37 eV in the theoretical curve aligning the main Cu $3d$ peak at -2.9 eV, there is general agreement for the DOS in the 0 to -8 eV range. The shoulder at -1.7 eV is well matched and the peak at -5.6 eV in the theoretical curve appears as a broad shoulder in the experimental data. However, there are two major disagreements. First, the calculation shows a finite DOS at the Fermi level due to the existence of the intrinsic hole population at the top of the VB, while the experimental data seem to suggest an edge at the gap. Second, the experimental data show additional "satellite" structures in the -10 to -12 eV range that are not reproduced by the calculation. The presence of these satellite structures has been attributed to the involvement of the two Cu $3d$ hole states in the one-electron removal spectrum, which cannot be adequately described by conventional one-electron band theory.[55,56] These two disagreements appear to come from the same source of strong correlation effects for states near the top of the VB. However, we should also be cautious in drawing such conclusions because photoemission experiments are very sensitive to surface conditions and sample contamination and, as such, a small DOS at E_F may not be detectable.

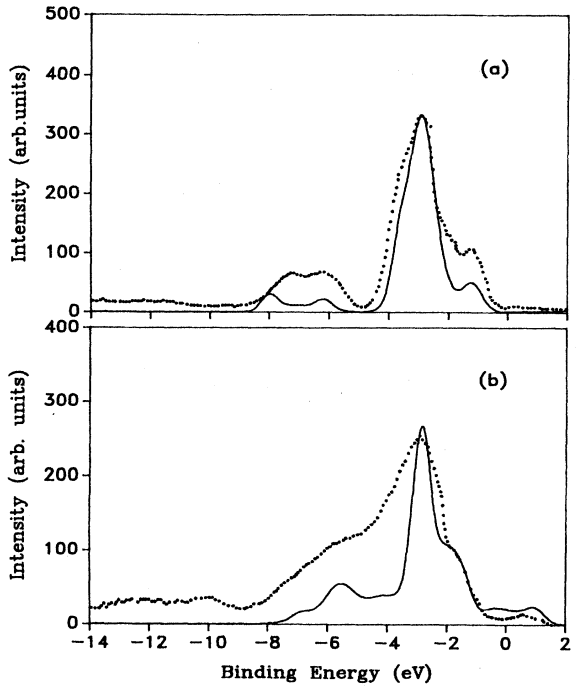

FIG. 13. Comparison of broadened valence-band DOS with experimental photoemission spectrum (Ref. 22, He II source): (a) Cu_2O and (b) CuO. See text for detail.

The broadened CB DOS for Cu_2O up to 18 eV is shown in Fig. 14(a), together with the BIS data from Ref. 22. It can be seen that the major structures at 2.9 eV can be roughly reproduced after a small downward shift of about 0.5 eV, thus again suggesting that the calculated gap should be smaller to account for this shift. The CB DOS shows much more structure than the experimental data even after a sizable smoothing of the calculated curve. Therefore the agreement between theory and experiment for the CB states in Cu_2O is not as impressive as for the VB shown in Fig. 12(a). With increased resolu-

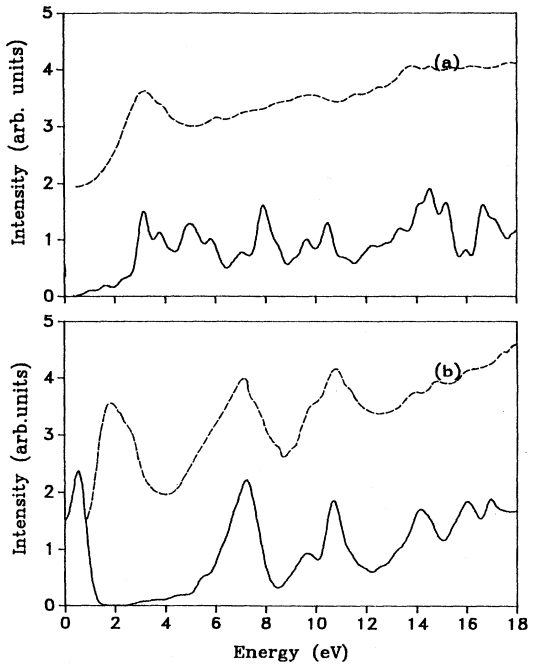

FIG. 14. Comparison of broadened conduction-band DOS with experimental BIS spectrum (Ref. 22): (a) Cu_2O and (b) CuO. See text for detail.

tion in the BIS spectra, some of the calculated structures may be better resolved.

In Fig. 13(b) we make a similar comparison for CuO without any shift in the calculated curve. With the exception of the leading peak, there is excellent agreement in all the peak structures from 4 up to 18 eV. The calculation fails to reproduce the leading peak at 1.9 eV. This is the same disagreement for states near the Fermi level discussed earlier in the VB spectra, and it reflects the general failure of the band calculation for states near E_F. Ironically, for the states high in the CB the agreement with experiment is better in CuO than in Cu_2O. It is difficult to understand why the structures in the CB for CuO are better resolved than for Cu_2O, especially when band theory is not expected to work well for CuO. If we identify the peak at 0.6 eV in the DOS of CuO where the intrinsic hole states lie as the leading experimental peak at 1.9 eV in the BIS spectra, the difference of 1.3 eV can probably be related to the degree of correlation for the states at the top of the VB. More realistic estimates should include the total-energy calculation[35] for both the ground state and the excited state for CuO. Unfortunately, such a calculation will be prohibitively difficult for a system like CuO. Thus, apart from the disagreement due to correlation effects of the *d*-shell hole in CuO, the overall agreement of the calculated band for CuO with experiment is better than expected.

VII. CONCLUSIONS

We have calculated the band structures and the interband optical properties of Cu_2O and CuO crystals using a first-principles method. This is the first time the band structure of CuO has been studied in detail. By comparing with different experimental measurements, it is safe to say that band theory can adequately predict the ground-state properties of the Cu_2O crystal. For CuO there is evidence that one-electron theory may not be adequate in interpreting the photoemission experiments, especially for the states near the top of the VB. It is argued that CuO may not be in exactly the same category as the transition-metal monoxides collectively known as Mott insulators. The nature of the intrinsic hole states at the top of the VB as calculated by one-electron local-density theory is not well understood and certainly warrants a more detailed study. Experimentally, CuO behaves like a semiconductor, yet the calculation shows it to be semiconductor-like with a Fermi surface below a well-defined gap. Many of the newly discovered high-T_c oxide superconductors have CuO as an important ingredient and show similar characteristics in their band structures, namely the existence of a semiconductor-like or semimetal-like gap, and a Fermi surface.[57] Therefore, further study of CuO oxide could add to the understanding of the normal-state properties of the superconducting oxides.

The calculation of interband optical conductivity is very revealing. There are no direct optical data on CuO available, but our calculated result is in line with the indirect photoelectrochemical measurement. Our theoretical calculations on CuO crystal will certainly be valuable for the interpretation of any future experimental data. In the case of Cu_2O the calculated spectrum is in very good agreement with the optical measurement if a shift in the energy scale is applied. This brings up an important point: The actual intrinsic gap in Cu_2O crystal is much smaller than the oft-quoted experimental gap that was deduced from the optical data. However, the strength of optical absorption is negligible for photon energies below the optical gap. This is because the symmetries of the wave functions at the Γ point are such that they are dipole-transition forbidden. The clarification of these two different gaps is important because many other experimental data may be interpreted differently. For example, the static dielectric constant ϵ_0 may have been derived from the optically measured excitonic levels and the assumed gap value. Our calculated ϵ_0 value as well as the intrinsic gap value are much smaller than the experimental values, but they still give a numerically correct value for the Rydberg constant as deduced from the excitonic spectra. It appears that our calculations have clarified long-standing confusion regarding some of the important fundamental constants in Cu_2O crystal. We conclude that the intrinsic gap in Cu_2O is of the order of 0.8 eV, while the dielectric constant should be of the order of 4.

ACKNOWLEDGMENTS

This work was supported by the U.S. Department of Energy under Grant No. DE-FG02-84ER45170.

*Permanent address: Department of Physics, Fudan University, Shanghai, People's Republic of China.
[1]M. Balkanski, Y. Petroff, and D. Trivich, Solid State Commun. **5**, 85 (1967).
[2]S. P. Tandon and J. P. Gupta, Phys. Status Solidi **37**, 43 (1970).
[3]J. L. Deiss, A. Daunois, and S. Nikitine, Solid State Commun. **8**, 521 (1970).
[4]R. S. Toth, R. Kilkson, and D. Trivich, Phys. Rev. **122**, 482 (1961).
[5]R. Kuzel and F. L. Weichman, Can. J. Phys. **48**, 1585 (1970).
[6]R. Kuzel and F. L. Weichman, Can. J. Phys. **48**, 2643 (1970).
[7]S. Minomura and H. G. Drickamer, J. Appl. Phys. **34**, 3043 (1963).
[8]A. L. Pranatis, J. Am. Ceram. Soc. **51**, 182 (1968).
[9]J. Hallberg and R. C. Hanson, Phys. Status Solidi **42**, 305 (1970).
[10]G. Vagnard and J. Washburn, J. Am. Ceram. Soc. **51**, 88 (1968).
[11]E. F. Gross, Suppl. Nuovo Cimento **3**, 12 (1956).
[12]E. F. Gross, Usp. Fiz. Nauk **26**, 433 (1962) [Sov. Phys.—Usp. **5**, 192 (1962)].
[13]J. L. Deiss, A. Daunois, and S. Nikitine, Solid State Commun. **7**, 1417 (1969).
[14]R. A. Forman, W. S. Brower, Jr., and H. S. Parker, Phys. Lett. **36A**, 395 (1971).
[15]K. Shindo, T. Goto, and T. Anzai, J. Phys. Soc. Jpn. **36**, 753 (1974).
[16]A. Z. Genack, H. Z. Cummins, M. A. Washington, and A. Compaan, Phys. Rev. B **12**, 2478 (1975).
[17]M. A. Washington, A. Z. Genack, H. Z. Cummins, R. H. Bruce, A. Compaan, and R. A. Forman, Phys. Rev. B **15**, 2145 (1977).
[18]D. P. Trauernicht and J. P. Wolfe, Phys. Rev. B **33**, 8506 (1986); **34**, 2561 (1986).
[19]C. Benndorf, H. Caus, B. Egert, H. Seidel, and F. Thieme, J. Electron. Spectrosc. Relat. Phenom. **19**, 77 (1980).
[20]M. R. Thuler, R. L. Benbow, and Z. Hurych, Phys. Rev. B **26**, 669 (1982).
[21]J. Drahokoupil, M. Polcik, and E. Pollert, Solid State Commun. **66**, 455 (1988).
[22]J. Ghijsen, L. H. Tjeng, J. van Elp, H. Eskes, J. Westerink, G. A. Sawatzky, and M. T. Czyżyk, Phys. Rev. B **38**, 11 322 (1988).
[23]B. X. Yang, J. M. Tranquada, and G. Shirane, Phys. Rev. B **38**, 174 (1988).
[24]C. P. Massolo, M. Renteria, J. Desimoni, and A. G. Bibiloni, Phys. Rev. B **37**, 4743 (1988); A. Bartos, W. Bolse, K. P. Lieb, and M. Uhrmacher, Phys. Lett. **130**, 177 (1988).
[25]J. G. Bednorz and K. A. Müller, Z. Phys. B **64**, 189 (1986); M. K. Wu *et al.*, Phys. Rev. Lett. **58**, 908 (1987); H. Maeda, Y. Tanaku, M. Futomi, and T. Asano, Jpn. J. Appl. Phys. **27**, 1209 (1988); Z. Z. Sheng and A. M. Herman, Nature (London) **332**, 55 138 (1988).
[26]See, for example, *Novel Superconductivity,* edited by S. A. Wolf and V. Z. Kresin (Plenum, New York, 1987).
[27]A. W. Sleight, Science **242**, 1519 (1988).
[28]V. P. Smirnov, Fiz. Tverd. Tela (Leningrad) **7**, 2856 (1965) [Sov. Phys.—Solid State **7**, 2312 (1966)]; **8**, 2519 (1966) [**8**, 2020 (1967)].
[29]J. P. Dahl and A. C. Switendick, J. Phys. Chem. Solids **27**, 931 (1966); J. Robertson, Phys. Rev. B **28**, 3378 (1983).
[30]L. Kleinman and K. Mednick, Phys. Rev. B **21**, 1549 (1980).
[31]R. J. Elliott, Phys. Rev. **108**, 1384 (1957).
[32]R. J. Elliott, Phys. Rev. **124**, 340 (1961).
[33]K. Terakura, A. R. Williams, T. Oguchi, and J. Kubler, Phys. Rev. Lett. **52**, 1830 (1984).
[34]K. Terakura, T. Oguchi, A. R. Williams, and J. Kubler, Phys. Rev. B **30**, 4734 (1984).
[35]M. R. Norman and A. J. Freeman, Phys. Rev. B **33**, 8896 (1986).
[36]P. Niggli, Z. Kristallogr. **57**, 253 (1922).
[37]G. Tunell, E. Posniak, and C. J. Ksanda, Z. Kristallogr. **90**, 120 (1935).
[38]S. Asbrink and L.-J. Norrby, Acta Crystallogr. Sec. B **26**, 8 (1970).
[39]P. J. Feibelmann, J. A. Appelbaum, and D. R. Hamann, Phys. Rev. B **20**, 1433 (1979).
[40]B. N. Harmon, W. Weber, and D. R. Hamann, Phys. Rev. B **34**, 5308 (1986).
[41]W. Y. Ching and B. N. Harmon, Phys. Rev. B **34**, 5305 (1986).
[42]W. Y. Ching, Y. Xu, G.-L. Zhao, K. W. Wong, and F. Zandiehnadem, Phys. Rev. Lett. **59**, 1333 (1987).
[43]G.-L. Zhao, Y. Xu, W. Y. Ching, and K. W. Wong, Phys. Rev. B **36**, 7203 (1987).
[44]Y. Xu, W. Y. Ching, and K. W. Wong, Phys. Rev. B **37**, 9773 (1988); W. Y. Ching, G. L. Zhao, Y. Xu, and K. W. Wong, in *Progress in High Temperature Superconductors Vol. 12: High Temperature Superconductivity and Other Related Topics,* edited by C. K. Chew, C. H. Lai, C. H. Oh, and K. K. Phua (World Scientific, Singapore, 1988), p. 58.; W. Y. Ching, G.-L. Zhao, Y. N. Xu, and K. W. Wong, Mod. Phys. Lett. B **3**, 263 (1989).
[45]G.-L. Zhao, W. Y. Ching, and K. W. Wong, J. Opt. Soc. Am. B **6**, 505 (1989).
[46]W. Y. Ching and C. C. Lin, Phys. Rev. B **12**, 5536 (1975); **16**, 2989 (1977).
[47]Y. N. Xu and W. Y. Ching, in *SiO_2 and Its Interfaces,* MRS Symp. Proc. No. 105, edited by S. T. Pantelides and G. Lucovsky (MRS, Pittsburgh, 1988), p. 181.
[48]G. Lehmann and M. Taut, Phys. Status Solidi **54**, 469 (1972); O. Jepsen and O. K. Anderson, Solid State Commun. **9**, 1763 (1971).
[49]R. S. Mulliken, J. Am. Chem. Soc. **77**, 887 (1954).
[50]G. Gilat and N. R. Bharatiya, Phys. Rev. B **12**, 3479 (1975); M. S. Methfessel, M. H. Boon, and F. M. Mueller, J. Phys. C **20**, 1069 (1987).
[51]L. Hardee and A. J. Bard, J. Electrochem. Soc. **124**, 215 (1977).
[52]F. P. Kottyberg and F. A. Benko, J. Appl. Phys. **53**, 1173 (1982).
[53]*The Oxide Handbook,* 2nd ed., edited by G. V. Samsonov (translated from the Russian by R. K. Johnston) (IFI/Plenum, New York, 1980).
[54]*Transition Metal Oxides: Crystal Chemistry, Phase Transitions and Related Aspects,* Nat. Bur. Stand. (U.S.) Ref. Data Ser. No. 49, edited by C. N. R. Rao and G. V. Subba Rao (U.S. GPO, Washington, D.C., 1974), p. 80.
[55]G. A. Sawatzky and J. W. Allen, Phys. Rev. Lett. **53**, 2339 (1984).
[56]A. Fujimori, F. Minami, and S. Sugano, Phys. Rev. B **29**, 5225 (1984).
[57]K. W. Wong and W. Y. Ching, Physica C **158**, 1 (1989); **158**, 15 (1989).